

Research Paper

Stabilization of Aerosolizable Nano-carriers by Freeze-Drying

Claudia B. Packhaeuser,¹ Kerstin Lahnstein,² Johannes Sitterberg,¹ Thomas Schmehl,² Tobias Gessler,² Udo Bakowsky,¹ Werner Seeger,² and Thomas Kissel^{1,3}

Received June 18, 2008; accepted August 19, 2008; published online October 8, 2008

Purpose. This study investigates the feasibility of freeze-drying aerosolizable nano-carriers (NC) by the use of different lyoprotective agents (LPA) and the influence of the freeze-drying on the physicochemical properties of these nano-carriers and on their aerosolization.

Methods. Nano-carriers were prepared from fast-degrading polymers, DMAPA(24)-PVAL-g-PLGA (1:7.5) and DEAPA(26)-PVAL-g-PLGA(1:10), and freeze-dried using increasing concentrations of different LPA. The hydrodynamic diameter, zeta potential and morphology (atomic force microscopy) of NC were characterized before and after freeze-drying. The ability to aerosolize using a jet nebulizer and an electronic micro-pump nebulizer was also investigated.

Results. Freeze-drying with LPA led to a decreased ζ -potential of NC and changes in size about 20 nm without alteration in shape, whereas lyophilizates without LPA were found to aggregate. While freeze-drying was positively affected by increasing concentrations, it was not influenced by the type of LPA. The possibility for aerosolization was not influenced by any LPA.

Conclusions. Freeze-drying with LPA is a suitable method to physically stabilize fast-degrading NC from aqueous suspensions without influencing the aerosolizability.

KEY WORDS: biodegradable; freeze-drying; lyoprotectant; nano-carrier; pulmonary delivery.

INTRODUCTION

Polymeric nanoparticles have been widely investigated as potential drug carriers (1). Nanoparticle formulations consist of small particles of 10–400 nm size, and are promising as drug carriers for the effective transport of poorly soluble therapeutics. When a drug is encapsulated in a nanoparticulate form, it can be delivered to the appropriate site, released in a controlled way and protected from undergoing premature degradation. The route of administration is an other important factor for therapeutic success. The respiratory tract has become an increasingly attractive route of application and has gained considerable interest in the field of nanomedicine (2,3). Several studies have shown that nanoparticles from different materials were internalized into human airway cells, such as A549 cells (4–7). These promising results have encouraged many groups to develop suitable formulations utilizing nanoparticulate carriers. One common method to deposit nano-sized drug carriers into the deep lung is the nebulization of particle suspensions (8). A number of nanoparticle formulations have been successfully used with common nebulizers, such as jet nebulizers, ultrasonic nebulizers and electronic pump nebulizers (9). One major

advantage of this method is that regardless of the aerodynamic properties of the nanoparticles themselves, alveolar deposition can be easily achieved by generating adequate droplet sizes (10). Alginate nanoparticles (11), poly(D,L-lactide-co-glycolide; PLGA) nanoparticles (12) and the particles prepared from branched polyesters designed in our labs (13) are a few examples. However, the aerosol droplet size distribution is an important variable in defining the efficiency of aerosolized drugs. In addition to deposition in the respiratory tract and biocompatibility, the research of nanoparticles for pulmonary drug delivery systems must also address the degradability of the drug carriers. Repeated application of slow- or non-degrading compounds may lead to accumulation in the lung, and cause inflammatory processes. It is also well known that patients with pulmonary restrictions show predisposition to the effects of inhaled particulate pollutants (14). For the above mentioned reasons, most common biodegradable polymers with prolonged biodegradation rates such as PLGA, are not suitable for application in the respiratory tract. One way to bypass this problem is to synthesize polymers with faster degradation rates that are not based on PLGA, such as biodegradable ether-anhydrides consisting of various ratios of sebacic acid (SA) and poly(ethylene glycol) PEG (15). Others have used chitosan/tripolyphosphate nanoparticles (16). Fast degrading polymers, composed of short PLGA chains grafted onto an amine-substituted poly(vinyl alcohol) backbone, have been designed for drug delivery, e.g., to the lung (17). Nano-carriers prepared from these polymers showed accelerated degradation compared to those of commercially available

¹ Department of Pharmaceutics and Biopharmacy, Philipps-University, Ketzerbach 63, 35032, Marburg, Germany.

² University of Giessen Lung Center (UGLC), 35392, Giessen, Germany.

³ To whom correspondence should be addressed. (e-mail: kissel@staff.uni-marburg.de)

PLGA (18). Since these polymers are degraded by hydrolysis, storage in aqueous suspensions is not possible. Freeze-drying has been reported as a powerful technique to stabilize a number of nanoparticulate compounds, such as nanoparticles prepared from PLGA (19), solid lipid nanoparticles (20,21), lipid-protamine-DNA complexes (22), oligonucleotide-poly-ethylenimine complexes (23) and silica nanoparticles (24). The mechanism of protection against aggregation by sugars and sugar alcohols was described as a retardation of molecular movement by the high viscosity of an amorphous lyoprotectant (25). Thus, the sugars glucose, lactose, sucrose, trehalose and the sugar alcohols mannitol and sorbitol were mainly used as lyoprotective agents (LPA).

The primary objective of this study was the freeze-drying of aerosolizable nano-carriers (NC) prepared from the fast-degrading polymers DMAPA(24)-PVAL-g-PLGA(1:7.5) and DEAPA(26)-PVAL-g-PLGA(1:10), and the investigation of the physicochemical characteristics of these NC during freeze-drying. Although, there was only little difference in the amine-modification, DMAPA or DEAPA and in the PLGA chain lengths, the influence of these parameters on the nano-carrier properties was also regarded. Therefore, we measured the hydrodynamic diameter of NC before and after freeze-drying by photon correlation spectroscopy (PCS). The ζ -potential of freshly prepared and freeze-dried NC was determined by laser Doppler anemometry (LDA). The influence of different lyoprotectants (sucrose, lactose, mannitol and glucose) on nano-carrier size and ζ -potential was investigated. Visualization of freshly prepared and freeze-dried NC was performed by atomic force microscopy (AFM). Additionally, the influence of the different LPAs on the aerosol droplet performance when nebulized with different types of nebulizers was investigated by laser diffraction and the effect on nebulizer output was determined.

MATERIALS AND METHODS

Two different polymers (Fig. 1) were used in this study: DEAPA(26)-PVAL-g-PLGA(1:10) according to Dailey *et al.* (13) and DMAPA(24)-PVAL-g-PLGA(1:7.5), both synthesized

as described earlier by Wittmar *et al.* (17). The amphiphilic polyesters were specifically designed for drug delivery to the lung and are comprised of short PLGA chains grafted onto an amine-substituted poly(vinyl alcohol) backbone. Carboxymethyl cellulose (Tylopur® C 600) was purchased from Clariant (Sulzbach, Germany). All other chemicals were of the highest analytical grade commercially available.

Preparation of Nano-carrier Suspensions

Nano-carrier suspensions were produced using a modified solvent displacement method, as described previously (26). To avoid artificial surfactants, the preparation was modified in the following manner: 5 mg polymer, dissolved in 1.5 ml acetone, were slowly injected into 5 ml distilled water containing 50 μ g CMC/mg polymer for DEAPA and DMAPA according to (13). After removal of the organic solvent by stirring the NC-suspensions for 3 h under reduced pressure, any evaporated water was replaced.

Freeze-drying

The stability of the nano-carrier suspensions during freeze-drying was investigated using increasing amounts of different lyoprotectants. Nano-carrier suspensions containing 1 mg/ml were mixed with glucose, sucrose, lactose or mannitol resulting in concentrations of 2.5%, 5% or 10%. Samples of 0.5–3.0 ml were frozen by placing in a -80°C cooler in Eppendorf-cups. Freeze-drying was performed using the lyophilizator Beta II (Christ, Osterode, Germany) which was pre-cooled to an ice condenser temperature of -50°C using the cryostat function prior to the transfer of the samples. Samples were dried for 7 days at a working pressure of 0.07 mbar corresponding to a condenser temperature of -46°C . Samples without lyoprotectants were freeze-dried as control. After freeze-drying, the nano-carrier suspensions were allowed to warm to room temperature, prior to resuspension in the original volume of ultra pure water and were vortexed or magnetically stirred if necessary. The particle size was determined by PCS, of both untreated and

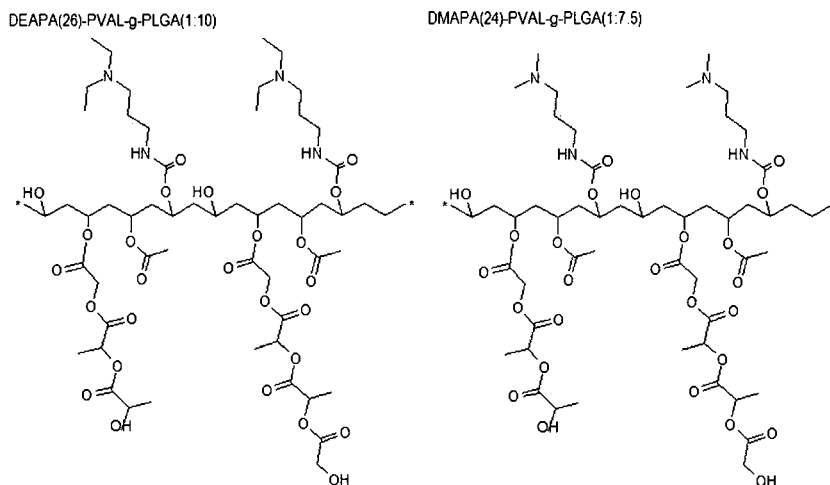


Fig. 1. Polymers as used in this study: DEAPA(26)-PVAL-g-PLGA(1:10), DEAPA and DMAPA(24)-PVAL-g-PLGA(1:7.5), DMAPA.

freeze-dried suspensions. All measurements were carried out in triplicate.

Nebulization of Nano-carrier Suspensions

Stability during Nebulization

Before and after freeze-drying, the stability of DMAPA (24)-PVAL-g-PLGA(1:7.5) and DEAPA(26)-PVAL-g-PLGA (1:10) nano-carriers during aerosolization was studied. Three different nebulizers were used: the jet nebulizer Pari® LC Star (Pari GmbH, Starnberg, Germany), the ultrasonic nebulizer Optineb® (Nebutech, Elsenfeld, Germany) and the electric micro-pump nebulizer Aeroneb® Pro (Aerogen, Mountain View, CA/USA). Briefly, samples of 2 ml suspension were nebulized with the Pari® LC Star, the Optineb® and the Aeroneb®. Nebulization was carried out at an airflow rate of 10 L/min for a total of 10 min or exhaustive nebulization of the reservoir, as previously described (6). Samples of the nebulized aerosol were collected by placing a glass microscope slide in front of the nebulizer mouthpiece and allowing the aerosol droplets to deposit on the glass. The resulting condensation fluid was collected in Eppendorf tubes for further analysis. For qualitative investigation of the stability of the nano-carrier suspensions, aliquots of the non-nebulized nano-carrier suspensions and of the suspensions after nebulization were added to a cuvette and the particle size and polydispersity index were measured using PCS as described below. All measurements were carried out in triplicate.

Nebulizer Performance

The mass median aerodynamic diameters (MMAD) of the aerosol droplets produced from the different nebulizers when filled with nano-carrier suspensions with or without lyoprotectant were determined using a HELOS Laser diffractometer (Sympatec, Clausthal-Zellerfeld, Germany). Nebulization was performed at an airflow rate of 10 L/min. Three milliliters of each suspension were directly nebulized in the laser beam. The mouthpiece was held 1 cm from the center of the laser beam. Isotonic NaCl solution (0.9% *m/v*) was used as control. The measurements were performed with aerosol concentrations of 5 to 30%, in 5 runs of 5 ms duration each and analyzed in MIE mode. The density of the aqueous suspensions and solutions, respectively, was set equal to that of pure water; thus, the MMAD is equal to the volume aerodynamic diameter.

Additionally, the nebulizers were weighed before and after each aerosolization experiment to calculate the nebulizer mass output. The resulting difference in weight was used to calculate the mass output in mg per minute.

Determination of the Viscosity

The kinematic viscosity of isotonic NaCl solution (0.9% *m/v*), the CMC solution (50 µg/ml) and the lyoprotectant solutions containing 10% (*w/v*) were measured using a capillary viscometer with a type II capillary, $k=1.022$ (Schott, Darmstadt, Germany) at a temperature of 22°C. All measurements were carried out in triplicate.

Characterization of Nano-carrier Suspensions

Photon Correlation Spectroscopy (PCS)

The effective hydrodynamic diameters were determined by PCS using a Malvern Nanosizer ZS ZEN3600 (Malvern Instruments, Herrenberg, Germany) at 25°C equipped with a 4 mW helium neon laser and the Malvern software. Samples were measured in disposable plastic cuvettes at 633 nm and a scattering angle of 173°. The viscosity (0.88 mPas) and the refractive index (1.33) of ultra pure water were used for data analysis of diluted samples. For analysis of samples containing LPA, the dispersant properties were adapted for sugar solutions with the viscosity set to 1.02 mPas and the refractive index set to 1.34. The DTS V. 4.20-software was used to calculate particle mean diameter (Z_{Ave}) and the width of the fitted Gaussian distribution, which is displayed as the polydispersity index (PDI). The PDI is calculated from a simple fit of a parabola to the correlation data. It is dimensionless and scaled such that values up to 0.20 indicate that the sample has a narrow size distribution. Since this analysis is not able to discern between broad and bimodal size distributions, samples displaying PDI values greater than 0.50 are probably not suitable for PCS (27). All measurements were carried out in triplicate. The accuracy of size measurements was routinely checked using reference polymer particles (Nanosphere Size Standards, 50, 100 and 200 nm, Duke Scientific Corp., Palo Alto, CA, USA).

Laser-Doppler-anemometry (LDA)

ζ-Potential measurements were carried out using the ZS ZEN3600 (Malvern Instruments, Herrenberg, Germany) at 25°C equipped with a 4 mW helium neon laser and the Malvern software. Electrophoretic light scattering was performed in disposable folded capillary cells at 633 nm. The DTS V. 4.20-software was used to calculate the average ζ-potential values from the data of multiple runs. The instrument was calibrated with a Malvern -50 mV transfer standard. All measurements were carried out in triplicate.

Atomic Force Microscopy

Imaging

Samples were prepared by placing a sample volume of 10 µL onto a glass which was modified with amino-silane to generate a positive surface charge. The particles were immobilized on the surface for a few minutes. The samples were washed twice with water and dried by compressed air. Atomic force microscopy was performed in dry state using a NanoWizard™ (JPK instruments, Berlin, Germany) in intermittent contact mode. Commercially available Si₃N₄ tips attached to I-type cantilevers (NCS 16, µ-mash, Estonia) were used. The cantilevers were about 125 µm long with a resonance frequency of about 200 Hz. The scan speed was proportional to the scan size and the scan frequency was between 0.5 and 1.0 Hz. Images were obtained by displaying the height signal of the cantilever in the retrace direction (resolution of 512×512 pixels).

Table 1. Particle Size, Polydispersity Index and, ζ -potential of Nano-carrier Formulations (DMAPA(24)-PVAL-g-PLGA(1:7.5)) Produced with Increasing Amounts of CMC

CMC ($\mu\text{g CMC/mg polymer}$)	Particle size (nm)	Polydispersity index	ζ -potential (mV)
0	55.6 \pm 3.1	0.339 \pm 0.097	3.2 \pm 6.6
5	214.2 \pm 33.8	0.093 \pm 0.080	5.5 \pm 7.6
10 ^a	830.4 \pm 125.1 ^a	0.720 \pm 0.129 ^a	-1.0 \pm 1.1 ^a
20	206.4 \pm 34.3	0.036 \pm 0.024	-19.4 \pm 1.7
50	185.1 \pm 10.5	0.140 \pm 0.051	-27.5 \pm 2.9
100	137.5 \pm 15.5	0.332 \pm 0.021	-28.5 \pm 3.8
200	169.3 \pm 7.3	0.453 \pm 0.112	-35.9 \pm 3.1
400	173.0 \pm 32.8	0.468 \pm 0.028	-33.1 \pm 1.6

^a Cases in which polymer precipitation and flocculation occurred.

Statistics

All measurements were carried out in triplicate and values are presented as the mean \pm S.D. unless otherwise noted. The software GraphPad InStat 3.00 (GraphPad Software, San Diego, CA, USA) was used to perform an unpaired *t*-test or a one-way analysis of variance (ANOVA) followed by a Student–Newman–Keuls multiple test, respectively, comparing the differences between the groups. The level of significance chosen for all tests was $P < 0.05$.

RESULTS

Stability during Nebulization

Eight nano-carrier formulations were generated with increasing amounts of CMC and were characterized with regard to particle size, polydispersity index, and ζ -potential

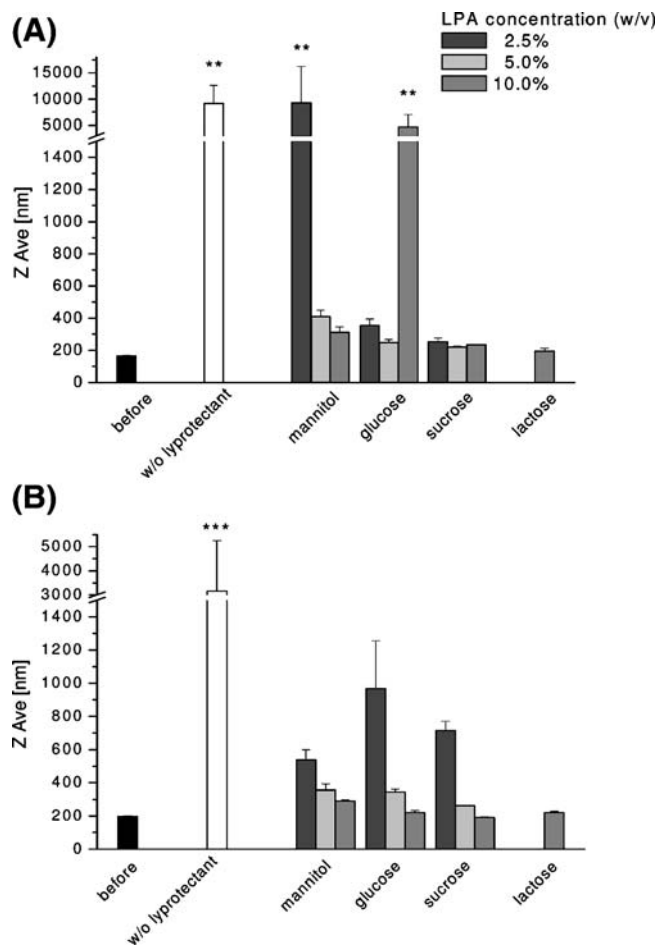


Fig. 3. Hydrodynamic diameter of (A) DMAPA and (B) DEAPA nano-carriers before and after freeze-drying with different lyoprotectants. Values are presented as the mean \pm S.D. ($n=3$). The asterisks denote statistically significant differences compared to untreated nano-carriers (** $P < 0.01$, *** $P < 0.05$).

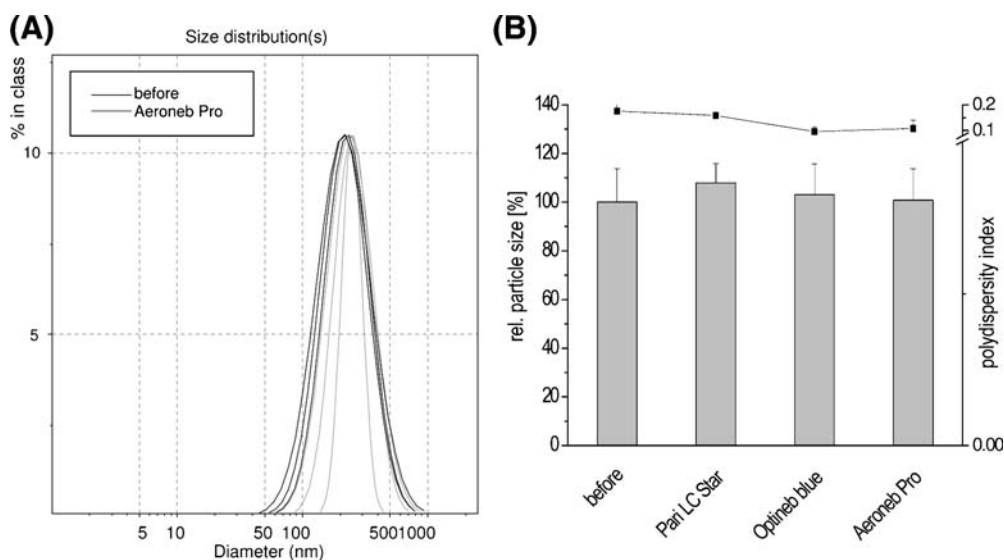


Fig. 2. Changes during nebulization of nano-carrier suspensions prepared from DMAPA with 50 $\mu\text{g CMC/mg}$ as stabilizing agent. (A) Size distributions of nano-carrier suspensions before and after nebulization with the Aeroneb Pro®. (B) Particle size and polydispersity index before and after nebulization with three different nebulizers. Values are presented as the mean \pm S.D. ($n=3$).

(Table I). Nano-carrier formation was highly dependent upon the ζ -potential of the nascent nano-carriers. Only particles displaying a positive or a pronounced negative charge were able to form stable suspensions, whereas formulations exhibiting a ζ -potential close to neutrality showed agglomeration. This was supported by polydispersity index measurements. While for negatively charged nanoparticles diameters decreased with increasing charge, the polydispersity index was only acceptable for a small range of ζ -potentials. These findings indicate nano-carrier instability when the CMC amount is too low or too high, respectively. Additionally, Dailey *et al.* (6) reported stability of comparable nano-carriers prepared from DEAPA during nebulization when negatively charged. Thus, nano-carrier suspensions with 50 μg CMC/mg polymer were chosen for further experiments.

Fig. 2(B) the particle size of nano-carriers in suspensions before nebulization and in the collected aerosols after nebulization are represented.

In the case of the ultrasonic nebulizer Optineb® the output was very poor (~ 65 mg/min) and no condensate could be collected. Thus, the size of the nano-carriers after nebulization was determined using the residual suspension in the nebulizer reservoir. Therefore, the ultrasonic nebulizer was not considered for further studies.

However, there was no change in particle size measured by PCS during aerosolization. In addition, the size distribution of each suspension was characterized by estimating the polydispersity index (Fig. 2(B)). The polydispersity index

ranged from 0.096 to 0.176. The broadest size distribution was found before nebulization (Fig. 2(A)), which suggested that the larger particles remained in the residual reservoir fluid or impacted on parts of the nebulizers. Independent of the applied nebulization technique, no differences in either particle size or polydispersity index were observed.

Effects of Freeze-drying on Nano-carrier Properties

Nano-carrier suspensions were freeze-dried with or without increasing amounts of lyoprotectants. After resuspension in water, the size of the nanoparticles and the ζ -potential were investigated. After freeze-drying the lyophilisates appeared voluminous and snow-like in the case of mannitol and lactose, condensed and salt-like in the case of sucrose and honey-like in the case of glucose.

Using the original volume of ultra pure water, lyophilisates prepared with mannitol and lactose were easily resuspended without further action, whereas lyophilisates prepared with sucrose and glucose needed to be magnetically stirred for 10 min, and preparations without lyoprotectants were not easily resuspended.

Fig. 3(A) and (B) show the results from the size measurements of untreated and freeze-dried nano-carrier suspensions prepared from DMAPA and DEAPA. In both cases the stabilizing effect of the LPAs increased with increasing concentration. Lactose and mannitol led to the most regular cakes, but mannitol offered the worst stabilization ability

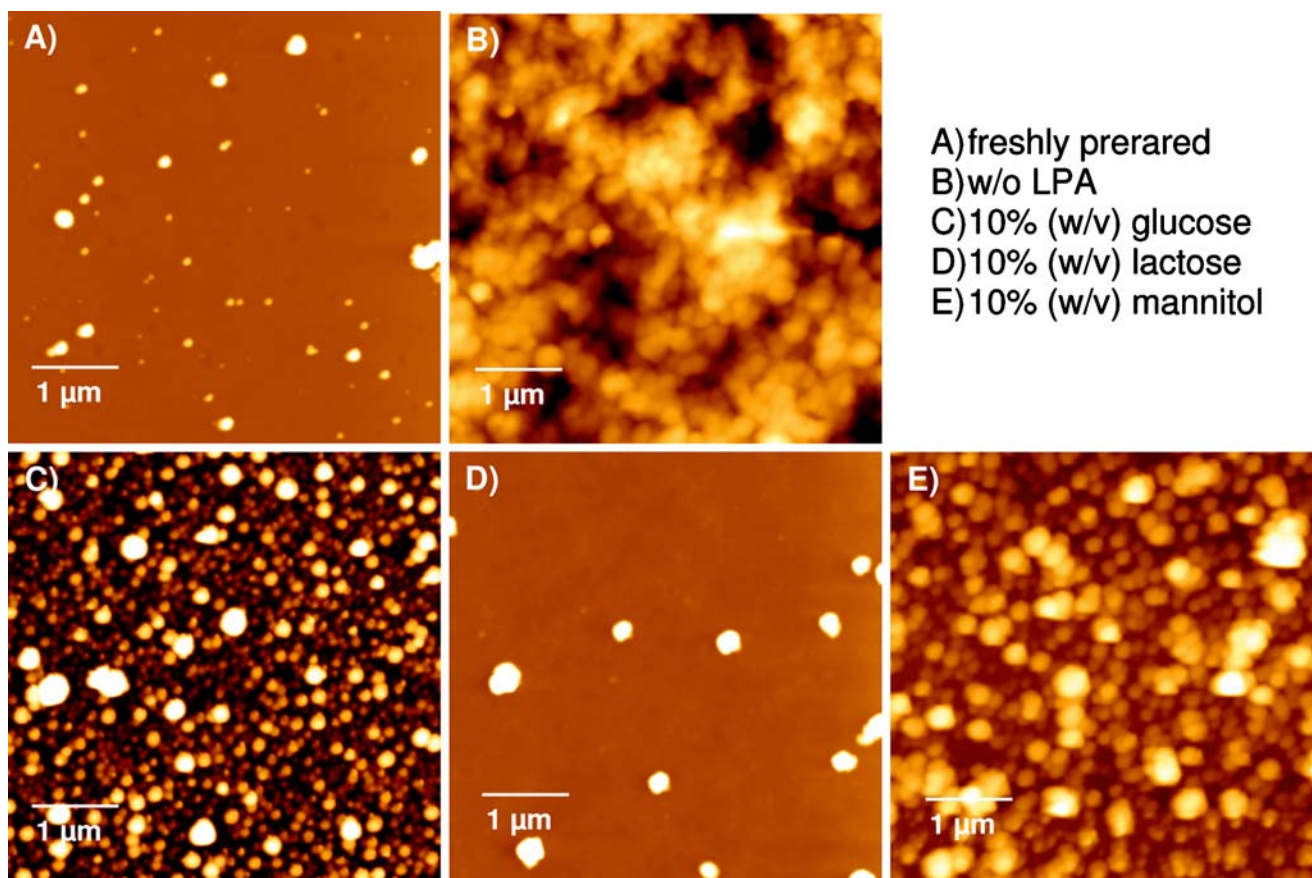


Fig. 4. AFM images of DEAPA nano-carriers before and after freeze-drying with or without lyoprotective agent (LPA).

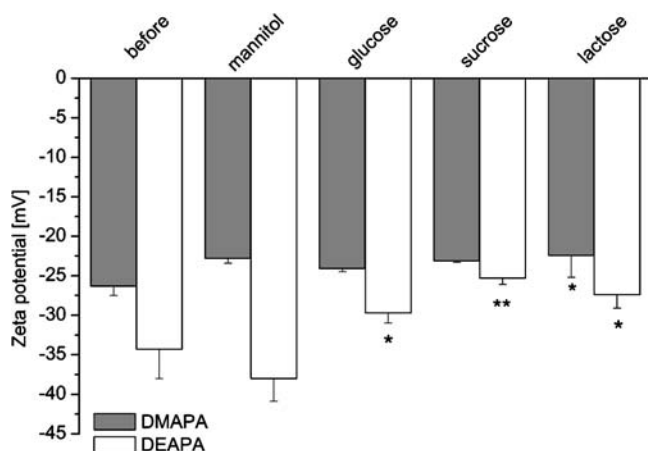


Fig. 5. ζ -potential of DMAPA and DEAPA nano-carriers before and after freeze-drying with different lyoprotectants at 10% (*w/v*). Values are presented as the mean \pm S.D. ($n=3$). The asterisks denote statistically significant differences compared to untreated nano-carriers (* $P < 0.05$, ** $P < 0.01$).

compared to the other additives. Only the addition of 10% (*w/v*) led to results comparable to the carbohydrates.

Another interesting finding was that glucose formed honey-like films instead of cakes. In the case of DMAPA-NC this led to a loss of size preservation at the highest concentration.

To obtain precise information of the size and shape before and after freeze-drying, we visualized nano-carriers prepared from DEAPA *via* AFM. Imaging was performed in dry state after washing the samples to avoid sugar crystal formation. Images of freshly prepared suspensions (Fig. 4(A)) showed homogeneously distributed nano-carriers. No aggregation of single nano-carriers was observed. When NC were

freeze-dried without the addition of LPA, huge aggregates could be found even after prolonging the resuspension time to 30 min under magnetic stirring (Fig. 4(B)). In contrast, images of rehydrated nano-carrier suspensions freeze-dried with 10% (*w/v*) of different lyoprotectants clearly demonstrated that freeze-drying had almost no influence on the NC size and shape (Fig. 4(C) and (D)). Only in the case of mannitol a few aggregates were observed (Fig. 4(E)), which is in agreement with the results from PCS.

Since the negative surface charge of DEAPA and DMAPA nano-carriers was found to be an important factor for the stability during aerosolization (28), we additionally investigated the influence of the freeze-drying step on the ζ -potential. The ζ -potential of suspensions containing NC prepared from DEAPA or DMAPA, respectively, were measured before and after freeze-drying with 10% (*w/v*) mannitol, glucose, sucrose or lactose. Overall, DEAPA-NC showed a higher surface charge of -35 mV compared to DMAPA-NC with -26 mV. The results presented in Fig. 5 show that freeze-drying had a decreasing effect about 5 mV on the surface charge of DMAPA-NC. This effect was slightly more pronounced for DEAPA-NC.

However, it was further investigated whether the change in ζ -potential had any impact on stability during nebulization. Nano-carrier suspensions resuspended after freeze-drying with 10% (*w/v*) LPA were nebulized either with the Pari® LC Star or the Aeroneb® and the condensed aerosols were collected to analyze the size and ζ -potential of the NC. In the case of DMAPA-NC freeze-dried with sucrose, an increase in the nano-carrier size as well as a decrease in the surface charge was observed for the electronic micro-pump nebulizer, while the jet nebulizer led only to an increase in nano-carrier size (Fig. 6). An increase in the ζ -potential was also found for DEAPA-NC when nebulized with lactose using the Pari® LC

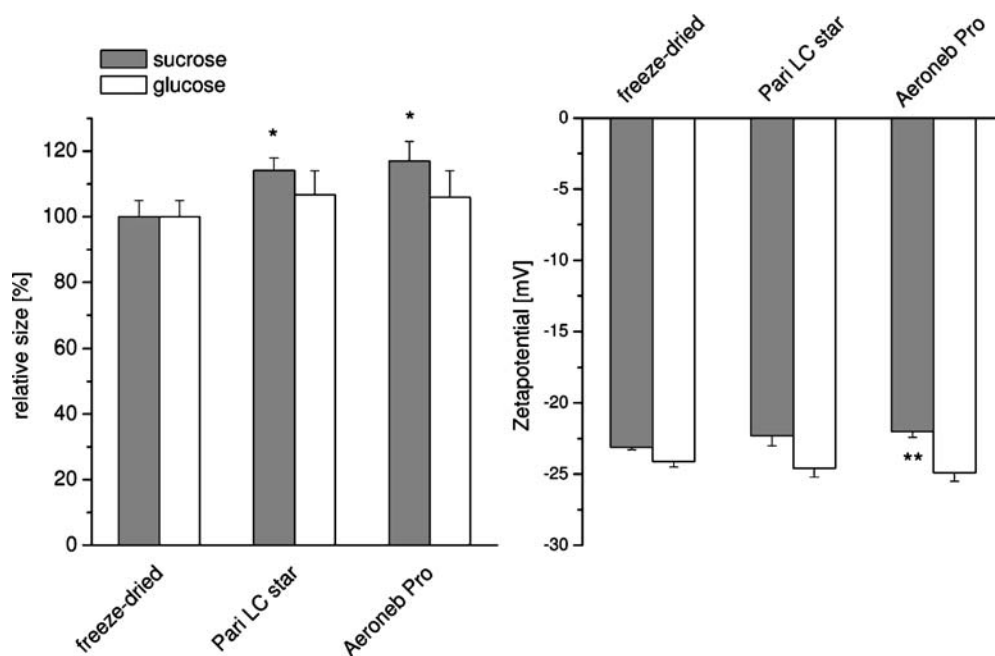


Fig. 6. Size and ζ -potential of freeze-dried DMAPA nano-carriers before and after nebulization with different lyoprotectants at 10% (*w/v*). Values are presented as the mean \pm S.D. ($n=3$). The asterisks denote statistically significant differences compared to nano-carriers before nebulization (* $P < 0.05$, ** $P < 0.01$).

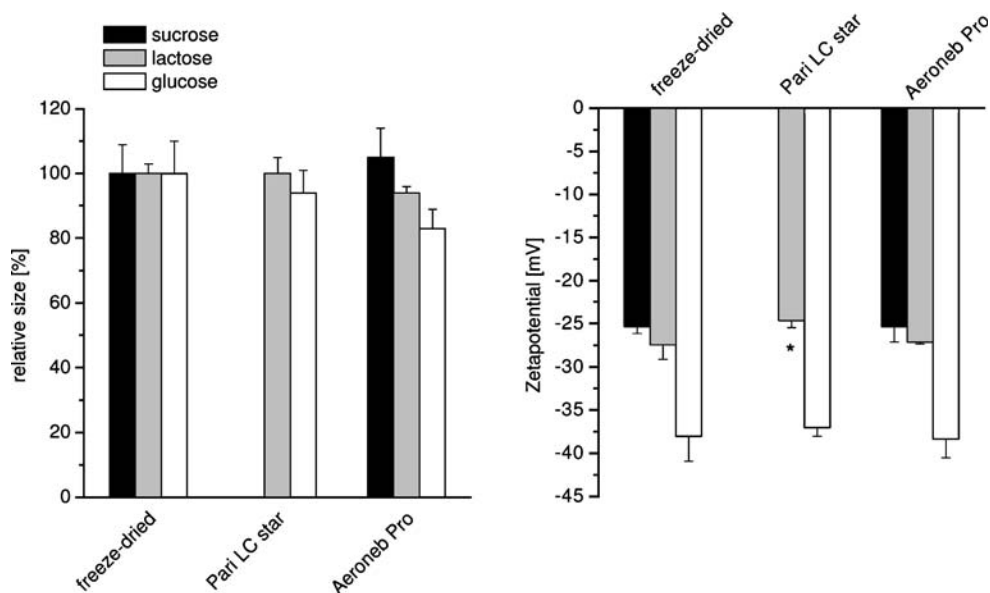


Fig. 7. Size and ζ -potential of freeze-dried DEAPA nano-carriers before and after nebulization with different lyoprotectants at 10% (*w/v*). Values are presented as the mean \pm S.D. ($n=3$). The asterisks denote statistically significant differences compared to nano-carriers before nebulization ($*P<0.05$).

star, but no significant change in nano-carrier size was found for all sugars and nebulizers studied (Fig. 7).

Table II displays the kinematic viscosities of the solutions nebulized in this study. As discussed above, for effective stabilization of the nano-carrier size, concentrations of 10% (*w/v*) lyoprotectants were necessary. These concentrations led to significant increase in viscosity compared to an isotonic sodium chloride solution. However, the nebulizer output was not influenced by the solution or suspension nebulized. The highest output was achieved with the jet air nebulizer Pari® LC Star, at 286 ± 10 mg/min. A similar output of 266 ± 20 mg/min was found with the electric micro-pump nebulizer Aeroneb®. As mentioned above, the output from the ultrasonic nebulizer Optineb® was very poor (65 mg/min), and it was not considered for further studies. The mass median aerodynamic diameters (MMAD) of aerosols generated from nano-carrier suspensions before freeze-drying and after resuspension of lyophilisates with 10% (*w/v*) of lactose, sucrose, or glucose were measured. The MMAD ranged from 4.06 ± 0.07 μm to 5.21 ± 0.05 μm , with slightly smaller sizes found for the jet nebulizer Pari® LC star aerosols compared to the electric micro-pump nebulizer Aeroneb®.

Table II. Kinematic Viscosities of Excipient Solutions

	Kinematic viscosity [mm^2/s]
0.9% NaCl	1.01 ± 0.02
50 $\mu\text{g/ml}$ CMC	1.12 ± 0.01 ***
10% lactose	1.24 ± 0.00 ***
10% sucrose	1.26 ± 0.01 ***
10% glucose	1.24 ± 0.01 ***
10% mannitol	1.26 ± 0.00 ***

Values are presented as the mean \pm S.D. ($n=3$).

The asterisks denote statistically significant differences compared to isotonic NaCl solution (*** $P<0.005$).

DISCUSSION

Sugar and sugar alcohols are known to stabilize proteins as well as nanoparticulates during freeze-drying. The mechanism of this protection against aggregation was described as a retardation of molecular movement by the high viscosity of an amorphous lyoprotectant and vitrification at the glass transition temperature (20,22,23,25,29). Reports on the influence of the lyoprotectant concentration on the stabilizing effect and resuspendibility have shown that concentrations of saccharides, disaccharides, and sugar alcohols above 1% (*w/v*) were necessary to effectively prevent aggregation and facilitate resuspension of nanoparticles (19,25,30). Consistent with literature, in this study only concentrations of sugars as high as 5–10% led to an effective physical stabilization of nano-carriers. With the sugar alcohol mannitol partially aggregation of the nanoparticles was observed even at those concentrations. This is in good agreement with the findings of other groups who had freeze-dried surface-charged nanoparticles. Lu *et al.* showed that mitoxantrone-loaded chitosan or bovine serum albumin (BSA) nanoparticles were best stabilized by the disaccharide lactose, whereas mannitol and sorbitol did not lead to resuspendibility (31). Sameti *et al.* also reported that 5% (*w/v*) mannitol did not effectively stabilize cationically modified silica nanoparticles (24). This was due to the fact that mannitol was found to crystallize during freeze-drying (32). The formation of hydrogen bonds between sugars or sugar alcohols and proteins is described as important factor for the stabilization of proteins during freeze-drying (33). Hence, an upper limit to the amount of protein to be embedded in a given amount of an amorphous sugar was postulated by Imamura *et al.* (29). Regarding the relatively weak hydrogen bond of crystalline compared to amorphous material as reported in (34), we assume that crystallization during the freezing step was responsible for the lower rate of protection by mannitol as compared to the glass forming carbohydrates, such as glucose

and sucrose, used in our study. The possibility to form hydrogen bonds might also explain the differences that we found for the stabilization of DMAPA- and DEAPA-NC. For maintaining the size of DEAPA-NC higher amounts of LPAs were necessary compared to DMAPA-NC. The shielding of the nitrogen-atom in DMAPA by methyl-groups is less pronounced than that by ethyl-groups in DEAPA. Hence, hydrogen bonding was assumed to be facilitated for the former polymer.

Using glucose as LPA led to a highly viscous matrix instead of a dry cake. Carbohydrates are known to change from crystalline to amorphous during freeze-drying, and to keep a certain moisture content during this process (35). Since the critical process step during freeze-drying regarding the physicochemical stability of nano-carriers is the freezing, we did not use a secondary drying step with warming the samples to room temperature for removing residual water. Thus, we assume that the conditions used in this study were insufficient to completely dry the glucose. Thus, the matrix did not fully vitrify leading to a loss of size preservation at the highest glucose concentration in the case of DMAPA-NC.

The differences in the ζ -potential values found for NC prepared from the two polymers, might be attributed to the higher degree of amine-modification in DEAPA compared to DMAPA. Hence, a higher amount of negatively charged CMC was associated with the nano-carrier surface, resulting in a decreased ζ -potential. The effect of lyoprotectants on the ζ -potential of nanoparticles is sparsely discussed in the literature. Only Sameti *et al.* postulated that LPAs such as trehalose, sorbitol, and glycerol partially shielded the nanoparticles and found some correlation between the reduction of the measurable surface potential and less permanent particle aggregation (24). Although no such correlation could be observed in our study, we assume that the reduction in the surface charge we found was due to partial covering of the nano-carrier surfaces by the LPAs. However, this is not regarded to be critical as only minor changes in NC properties during nebulization were observed. The increase of solution concentration during nebulization using different types of nebulizers has been described in literature (36,37). We assume that this increase in concentration led to a more pronounced shielding of the nano-carrier surface, resulting in a decrease in ζ -potential. The increased size might be due to partial crystallization of sucrose. Disaccharides, such as sucrose and lactose could be crystallized from solutions by decreasing the temperature (38,39). Steckel *et al.* described a decrease in aerosol temperature during nebulization using jet nebulizers (37). This well known decreasing temperature is due to the evaporation of solvent during nebulization and although it has not yet been reported, it is assumed to occur in electronic micro-pump nebulizers, too. In addition, Imamura *et al.* (29) found sucrose to partially crystallize during rehydration. Although some of the effects showed statistical significance, the stability of nano-carrier suspensions during nebulization is still evident by the maintained negative surface charge and the size did not exceed the 260 nm threshold of macrophage detection (40).

In conclusion, lactose, which is a well described and widely accepted excipient in powder inhalative formulations (41,42), was found to offer the best possibilities to protect nanoparticles against aggregation during freeze-drying and to prepare dry and easy to recover formulations. This may also

offer the opportunity to generate dry inhalable powders of lactose with an incorporated nano-carrier, which so far has been achieved by an alternative formulation step, i.e., spray-drying nanoparticles into sugary microparticles (16,43,44).

While the preservation of the nano-carrier properties is requisite to ensure the functionality of the drug delivery system, the properties of the aerosol is essential for its deposition in the airways (10). Regardless of the performance of a freeze-drying step and independent from the LPA used, aerosols generated from nano-carrier suspensions showed all MMADs in the range of 1–5 μm , which is suitable for central and deep lung deposition.

CONCLUSION

The results of this study demonstrate that freeze-drying is a very effective technique to produce physically stable nano-carrier formulations consisting of the fast-degrading polymers DMAPA(24)-PVAL-g-PLGA(1:7.5) and DEAPA(26)-PVAL-g-PLGA(1:10). Sizes of the nano-carriers were only marginally increased by the freeze-drying process, and the nano-carrier sizes did not exceed the 260 nm threshold of macrophage detection. AFM images showed that NC shape was not influenced by the freeze-drying, regardless of the lyoprotectant used. A slight decrease in surface charge was found, but this had no impact on the feasibility of aerosolizing the nano-carrier suspensions with common nebulizers. The mass median aerodynamic diameters (MMAD) of aerosols generated from nano-carrier suspensions independent from a performed freeze-drying were all in the range of 1–5 μm , which is suitable for central and deep lung deposition. We conclude that freeze-drying allows the stabilization of aerosolizable nano-carriers for controlled pulmonary delivery with regard to their physicochemical properties. However, to obtain long term stability during storage, an additional drying step to remove residual water might be necessary. Prospectively, the determination of the molecular weights and the glass transition temperatures of the polymers at the different process steps should be employed to investigate the stability against degradation.

ACKNOWLEDGEMENTS

Financial support of this work by Deutsche Forschungsgemeinschaft (DFG Forschergruppe 627) is gratefully acknowledged. We thank Klaus Keim, Department of Pharmaceutics and Biopharmacy, Philipps-Universität Marburg for the assistance with the artwork.

REFERENCES

1. D. A. Groneberg, M. Giersig, T. Welte, and U. Pison. Nano-particle-based diagnosis and therapy. *Curr. Drug Targets.* 7:643–648 (2006) doi:10.2174/138945006777435245.
2. D. A. Groneberg, C. Witt, U. Wagner, K. F. Chung, and A. Fischer. Fundamentals of pulmonary drug delivery. *Respir. Med.* 97:382–387 (2003) doi:10.1053/rmed.2002.1457.

3. U. Pison, T. Welte, M. Giersig, and D. A. Groneberg. Nano-medicine for respiratory diseases. *Eur. J. Pharmacol.* **533**:341–350 (2006) doi:10.1016/j.ejphar.2005.12.068.
4. M. Brzoska, K. Langer, C. Coester, S. Loitsch, T. O. Wagner, and C. Mallinckrodt. Incorporation of biodegradable nanoparticles into human airway epithelium cells—in vitro study of the suitability as a vehicle for drug or gene delivery in pulmonary diseases. *Biochem. Biophys. Res. Commun.* **318**:562–570 (2004) doi:10.1016/j.bbrc.2004.04.067.
5. M. Bivas-Benita, S. Romeijn, H. E. Junginger, and G. Borchard. PLGA-PEI nanoparticles for gene delivery to pulmonary epithelium. *Eur. J. Pharm. Biopharm.* **58**:1–6 (2004) doi:10.1016/j.ejpb.2004.03.008.
6. L. A. Dailey, E. Kleemann, M. Wittmar, T. Gessler, T. Schmehl, C. Roberts, W. Seeger, and T. Kissel. Surfactant-free, biodegradable nanoparticles for aerosol therapy based on the branched polyesters, DEAPA-PVAL-g-PLGA. *Pharm. Res.* **20**:2011–2020 (2003) doi:10.1023/B:PHAM.000008051.94834.10.
7. S. Azarmi, X. Tao, H. Chen, Z. Wang, W. H. Finlay, R. Loebenberg, and W. H. Roa. Formulation and cytotoxicity of doxorubicin nanoparticles carried by dry powder aerosol particles. *Int. J. Pharm.* **319**:155–161 (2006) doi:10.1016/j.ijpharm.2006.03.052.
8. P. G. Rogueda, and D. Traini. The nanoscale in pulmonary delivery. Part 2: formulation platforms. *Expert Opin. Drug Deliv.* **4**:607–620 (2007) doi:10.1517/17425247.4.6.607.
9. M. Knoch, and M. Keller. The customised electronic nebuliser: a new category of liquid aerosol drug delivery systems. *Expert Opin. Drug Deliv.* **2**:377–390 (2005) doi:10.1517/17425247.2.2.377.
10. P. G. Rogueda, and D. Traini. The nanoscale in pulmonary delivery. Part 1: deposition, fate, toxicology and effects. *Expert Opin. Drug Deliv.* **4**:595–606 (2007) doi:10.1517/17425247.4.6.595.
11. A. Zahoor, S. Sharma, and G. K. Khuller. Inhalable alginate nanoparticles as antitubercular drug carriers against experimental tuberculosis. *Int. J. Antimicrob. Agents.* **26**:298–303 (2005) doi:10.1016/j.ijantimicag.2005.07.012.
12. R. Pandey, A. Sharma, A. Zahoor, S. Sharma, G. K. Khuller, and B. Prasad. Poly (DL-lactide-co-glycolide) nanoparticle-based inhalable sustained drug delivery system for experimental tuberculosis. *J. Antimicrob. Chemother.* **52**:981–986 (2003) doi:10.1093/jac/dkg477.
13. L. A. Dailey, T. Schmehl, T. Gessler, M. Wittmar, F. Grimminger, W. Seeger, and T. Kissel. Nebulization of biodegradable nanoparticles: impact of nebulizer technology and nanoparticle characteristics on aerosol features. *J. Contr. Rel.* **86**:131–144 (2003) doi:10.1016/S0168-3659(02)00370-X.
14. G. Oberdorster. Pulmonary effects of inhaled ultrafine particles. *Int. Arch. Occup. Environ. Health.* **74**:1–8 (2001) doi:10.1007/s004200000185.
15. J. Fiegel, J. Fu, and J. Hanes. Poly(ether-anhydride) dry powder aerosols for sustained drug delivery in the lungs. *J. Contr. Rel.* **96**:411–423 (2004) doi:10.1016/j.jconrel.2004.02.018.
16. A. Grenha, B. Seijo, and C. Remunan-Lopez. Microencapsulated chitosan nanoparticles for lung protein delivery. *Eur. J. Pharm. Sci.* **25**:427–437 (2005) doi:10.1016/j.ejps.2005.04.009.
17. M. Wittmar, F. Unger, and T. Kissel. Biodegradable brushlike branched polyesters containing a charge-modified poly(vinyl alcohol) backbone as a platform for drug delivery systems: synthesis and characterization. *Macromolecules.* **39**:1417–1424 (2006) doi:10.1021/ma051837n.
18. C. Packhaeuser, M. Wittmar, J. Sitterberg, T. Gessler, T. Schmehl, U. Bakowsky, W. Seeger, and T. Kissel. Fast-degrading nanocarriers for pulmonary drug delivery, *Proceedings—33rd Annual Meeting & Exposition of the Controlled Release Society*, Vol. 2006, Vienna, Austria, 2006, pp. Abstract # 341.
19. Y. I. Jeong, Y. H. Shim, C. Kim, G. T. Lim, K. C. Choi, and C. Yoon. Effect of cryoprotectants on the reconstitution of surfactant-free nanoparticles of poly(DL-lactide-co-glycolide). *J. Microencapsul.* **22**:593–601 (2005) doi:10.1080/02652040500162659.
20. S. Kamiya, Y. Nozawa, A. Miyagishima, T. Kurita, Y. Sadzuka, and T. Sonobe. Physical characteristics of freeze-dried griseofulvin-lipids nanoparticles. *Chem. Pharm. Bull. (Tokyo).* **54**:181–184 (2006) doi:10.1248/cpb.54.181.
21. E. Vighi, B. Ruozzi, M. Montanari, R. Battini, and E. Leo. Redispersible cationic solid lipid nanoparticles (SLNs) freeze-dried without cryoprotectors: characterization and ability to bind the pEGFP-plasmid. *Eur. J. Pharm. Biopharm.* **67**:320–328 (2007) doi:10.1016/j.ejpb.2007.02.006.
22. B. Li, S. Li, Y. Tan, D. B. Stolz, S. C. Watkins, L. H. Block, and L. Huang. Lyophilization of cationic lipid-protamine-DNA (LPD) complexes. *J. Pharm. Sci.* **89**:355–364 (2000) doi:10.1002/(SICI)1520-6017(200003)89:3<355::AID-JPS7>3.0.CO;2-H.
23. C. Brus, E. Kleemann, A. Aigner, F. Czubyko, and T. Kissel. Stabilization of oligonucleotide–polyethylenimine complexes by freeze-drying: physicochemical and biological characterization. *J. Contr. Rel.* **95**:119–131 (2004) doi:10.1016/j.jconrel.2003.10.021.
24. M. Sameti, G. Bohr, M. N. Ravi Kumar, C. Kneuer, U. Bakowsky, M. Nacken, H. Schmidt, and C. M. Lehr. Stabilisation by freeze-drying of cationically modified silica nanoparticles for gene delivery. *Int. J. Pharm.* **266**:51–60 (2003) doi:10.1016/S0378-5173(03)00380-6.
25. W. Abdelwahed, G. Degobert, S. Stainmesse, and H. Fessi. Freeze-drying of nanoparticles: formulation, process and storage considerations. *Adv. Drug Del. Rev.* **58**:1688–1713 (2006) doi:10.1016/j.addr.2006.09.017.
26. T. Jung, A. Breitenbach, and T. Kissel. Sulfobutylated poly(vinyl alcohol)-graft-poly(lactide-co-glycolide)s facilitate the preparation of small negatively charged biodegradable nanospheres. *J. Control. Release.* **67**:157–169 (2000) doi:10.1016/S0168-3659(00)00201-7.
27. R. H. Müller, and R. Schuhmann. *Teilchengrößenmessung in der Laborpraxis*. Wissenschaftliche Verlagsgesellschaft, Stuttgart, 1996.
28. L. A. Dailey, T. Schmehl, T. Gessler, M. Wittmar, F. Grimminger, W. Seeger, and T. Kissel. Nebulization of biodegradable nanoparticles: impact of nebulizer technology and nanoparticle characteristics on aerosol features. *J. Control. Release.* **86**:131–144 (2003) doi:10.1016/S0168-3659(02)00370-X.
29. K. Imamura, M. Iwai, T. Ogawa, T. Sakiyama, and K. Nakanishi. Evaluation of hydration states of protein in freeze-dried amorphous sugar matrix. *J. Pharm. Sci.* **90**:1955–1963 (2001) doi:10.1002/jps.1146.
30. A. M. Layre, P. Couvreur, J. Richard, D. Requier, N. Eddine Ghermani, and R. Gref. Freeze-drying of composite core-shell nanoparticles. *Drug Dev. Ind. Pharm.* **32**:839–846 (2006) doi:10.1080/03639040600685134.
31. B. Lu, S. B. Xiong, H. Yang, X. D. Yin, and R. B. Zhao. Mitoxantrone-loaded BSA nanospheres and chitosan nanospheres for local injection against breast cancer and its lymph node metastases. I: formulation and in vitro characterization. *Int. J. Pharm.* **307**:168–174 (2006) doi:10.1016/j.ijpharm.2005.09.037.
32. C. Telang, L. Yu, and R. Suryanarayanan. Effective inhibition of mannitol crystallization in frozen solutions by sodium chloride. *Pharm. Res.* **20**:660–667 (2003) doi:10.1023/A:1023263203188.
33. W. Wang. Lyophilization and development of solid protein pharmaceuticals. *Int. J. Pharm.* **203**:1–60 (2000) doi:10.1016/S0378-5173(00)00423-3.
34. X. C. Tang, M. J. Pikal, and L. S. Taylor. The effect of temperature on hydrogen bonding in crystalline and amorphous phases in dihydropyridine calcium channel blockers. *Pharm. Res.* **19**:484–490 (2002) doi:10.1023/A:1015199713635.
35. M. G. Fakes, M. V. Dali, T. A. Haby, K. R. Morris, S. A. Varia, and A. T. M. Serajuddin. Moisture sorption behavior of selected bulking agents used in lyophilized products. *PDA J Pharm Sci Technol.* **54**:144–149 (2000).
36. R. W. Niven, A. Y. Ip, S. J. Prestrelski, and T. Arakawa. Some factors associated with the ultrasonic nebulization of proteins. *Pharm. Res.* **12**:53–59 (1995) doi:10.1023/A:1016282502954.
37. H. Steckel, and F. Eskandar. Factors affecting aerosol performance during nebulization with jet and ultrasonic nebulizers. *Eur. J. Pharm. Sci.* **19**:443–455 (2003) doi:10.1016/S0928-0987(03)00148-9.
38. K. Kawakami, K. Miyoshi, N. Tamura, T. Yamaguchi, and Y. Ida. Crystallization of sucrose glass under ambient conditions: evaluation of crystallization rate and unusual melting behavior of resultant crystals. *J. Pharm. Sci.* **95**:1354–1363 (2006) doi:10.1002/jps.20458.

39. X. M. Zeng, G. P. Martin, C. Marriott, and J. Pritchard. The influence of crystallization conditions on the morphology of lactose intended for use as a carrier for dry powder aerosols. *J. Pharm. Pharmacol.* **52**:633–643 (2000) doi:10.1211/0022357001774462.
40. R. W. Niven. Delivery of biotherapeutics by inhalation aerosol. *Crit. Rev. Ther. Drug Carrier Syst.* **12**:151–231 (1995).
41. H.-K. Chan, and N. Y. K. Chew. Novel alternative methods for the delivery of drugs for the treatment of asthma. *Adv. Drug Del. Rev.* **55**:793–805 (2003) doi:10.1016/S0169-409X(03)00078-4.
42. P. Baldrick, and D. G. Bamford. A toxicological review of lactose to support clinical administration by inhalation. *Food Chem. Toxicol.* **35**:719–733 (1997) doi:10.1016/S0278-6915(97)00041-0.
43. J. O. Sham, Y. Zhang, W. H. Finlay, W. H. Roa, and R. Lobenberg. Formulation and characterization of spray-dried powders containing nanoparticles for aerosol delivery to the lung. *Int. J. Pharm.* **269**:457–467 (2004) doi:10.1016/j.ijpharm.2003.09.041.
44. R. O. Cook, R. K. Pannu, and I. W. Kellaway. Novel sustained release microspheres for pulmonary drug delivery. *J Control. Release.* **104**:79–90 (2005) doi:10.1016/j.jconrel.2005.01.003.